Applied Thermal Engineering 175 (2020) 115385

Contents lists available at ScienceDirect

Applied Thermal Engineering

journal homepage: www.elsevier.com/locate/apthermeng

Parametric study on the thermal performance enhancement of a thermosyphon heat pipe using covalent functionalized graphene nanofluids

Emad Sadeghinezhad[a,1], Amir Reza Akhiani[b,1], Hendrik Simon Cornelis Metselaar[b], Sara Tahan Latibari[e], Mehdi Mehrali[d], Mohammad Mehrali[e,*]

[a] School of Minerals and Energy Resources, UNSW Sydney, Australia
[b] Centre of Advanced Materials, Department of Mechanical Engineering, University of Malaya, 50603 Kuala Lumpur, Malaysia
[d] Department of Mechanical Engineering, Section of Manufacturing Engineering, Technical University of Denmark, 2800 Kgs., Lyngby, Denmark
[e] Faculty of Engineering Technology, Laboratory of Thermal Engineering, University of Twente, Enschede 7500 AE, The Netherlands

HIGHLIGHTS

- Highly dispersible graphene nanofluids prepared using covalent functionalization.
- The heat transfer and thermal conductance potency promoted by by graphene nanosheets.
- A trade-off between filling ratio, tilt angle and performance were identified.
- The apparent enhancements of effective thermal conductivity were 105 at φ = 5%.
- The reduction in thermal resistance was 26.4% for prepared nanofluid at φ = 5%.

ARTICLE INFO

Keywords:
Graphene nanofluid
Heat pipe
Thermal efficiency
Thermal properties
Heat transfer coefficient
Filling ratio

ABSTRACT

Heat transfer characteristics of copper sintered heat pipe explored using a modified graphene nanoplatelets (GNP)-containing nanofluid with great dispersion stability as a novel working fluid. Firstly, a water dispersible GNP with specific desire was synthesized by the reaction of GNP sheets with the diazonium salt (DS) of sodium 4-aminoazobenzene-4-sulfonate. An X-ray photoelectron spectroscopy (XPS) test shown successful covalent functionalization of GNP using DS which provided special water dispersibility characteristics. The results indicate that the thermal conductivity enhancement was up to 17% by adding modified GNP sheets in the base fluid. It also, exhibited a maximum sedimentation of 16% after 840 hrs. Further research works were carried on thermal performance of heat pipe by varying nanofluid concentrations, filling ratio, input heating powers and inclination angles of heat pipes. The results proof that the maximum enhancements of the effective thermal conductivity and reduction in thermal resistance for purposed nanofluid atφ = 5% were 105% and 26.4%, respectively. Moreover, these good features of the GNP/DS nanofluid make it a very promising working fluid to enhance the thermal performance and efficiency of the current heat pipe systems.

1. Introduction

The demand for energy saving is increasing at an enormous rate as the economy of the countries is growing. Apart from them, developing a highly efficient and low-cost heat transfer device such as heat pipe system is becoming more important due to the development of industries. Typical heat pipes have played an important role in the heat dissipation and the thermal management systems [1–3]. A heat pipe as a condensation and evaporation device could transfer latent heat of vapor that flow from the evaporator section to the condenser section over long distances with negligible heat loss. Also, heat pipe could be known as a high efficient heat transfer system and it can transfer the thermal energy including heat from a higher temperature (evaporation) to a lower temperature (condenser) heat source [4,5]. In the heat pipe systems, the heat energy can transfer through the solid casing material of the heat pipe and it absorbs by the working fluid through conduction. These phenomena could explain as the working fluid vaporizes inside the vessel and it is saturated two phase (liquid and vapor) cycle and

* Corresponding author.
E-mail address: m.mehrali@utwente.nl (M. Mehrali).
[1] The first two authors have contributed to this research work equally.

https://doi.org/10.1016/j.applthermaleng.2020.115385
Received 27 January 2020; Received in revised form 25 March 2020; Accepted 20 April 2020
Available online 21 April 2020

Table 1
List of some research on graphene nanofluids using as working fluid.

Researcher	Nanofluid	Heat pipe specification	Input power (W)	Thermal resistance reduction
Kim and Bang [6]	GO nanofluid	Stainless steel tube (316L) d = 22 mm L = 1000 mm	100–350	About 25%
Asirvatham, Wongwises and Babu [24]	Graphene/acetone nanofluid	Borosilicate glass d = 12 mm L = 310 mm	10–50	Up to 70.3%
Mehrali, Sadeghinezhad, Azizian, Akhiani, Tahan Latibari, Mehrali and Metselaar [10]	Nitrogen-doped graphene nanofluid	Grooved copper tube d = 10 mm L = 300 mm	10–120	Up to 99%
Tharayil, Asirvatham, Ravindran and Wongwises [25]	Graphene/distilled water nanofluid	Copper L = 404 mm	20–380	Up to 29.9%
Su, Zhang, Han and Guo [26]	GO nanofluid	Copper tube d = 2 mm	10–100	Up to 15%

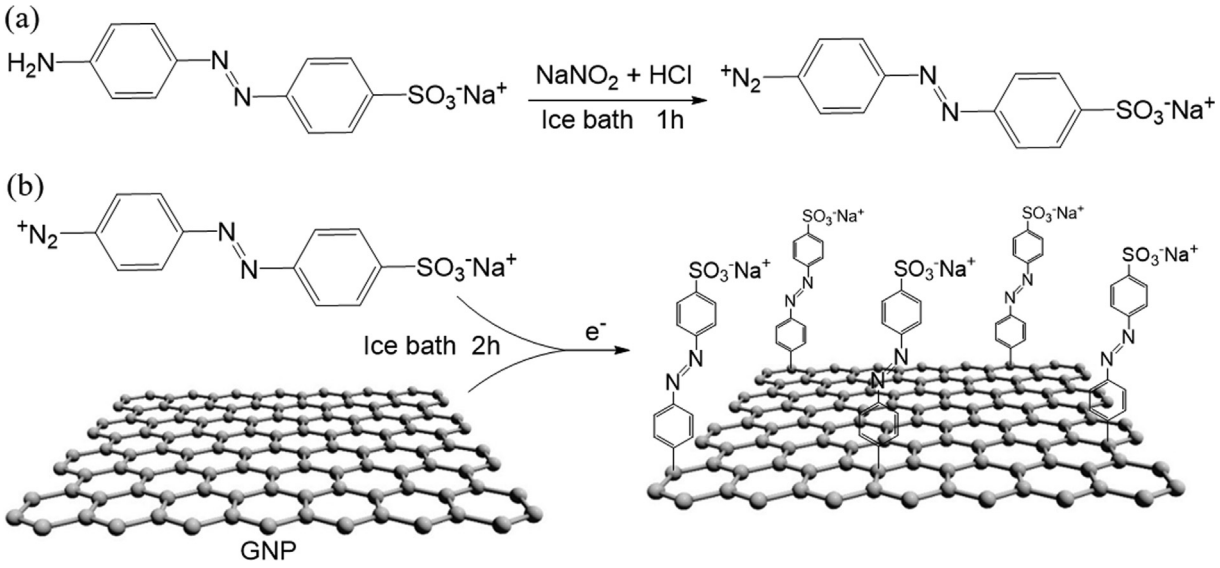

Fig. 1. Functionalization mechanism of the GNP samples (a) formation of diazonium cation, (b) reduction of diazonium by GNP.

Fig. 2. Water dispersibility of DS-GNP.

additional energy that added to the system will go into latent heat of vaporization [6–9].

Three main components are important in the design of a heat pipe, including container materials (Some materials are more effective conductors for a heat transfer capacity than the others), the working fluid and the wick (sintered, groove and mesh). A typical heat pipe system has three sections including a heat addition section (evaporator), an adiabatic section (ideally no heat loss) and a heat rejection section (condenser) [10,11]. The heat pipes have been used in a wide range of applications due to the following reasons [12]:

1- The condenser and evaporator section of a heat pipe can function independently.
2- The heat pipes can be manufactured with any size and shape base on the design requirement.
3- The heat pipes have a range of operating temperature from 4 to 3000 K.
4- The heat pipe has a different heat fluxes capacity that will allow it to function properly.

A heat pipe system can deliver high effective thermal conductivity from one to other ends and could reach a higher level of temperature

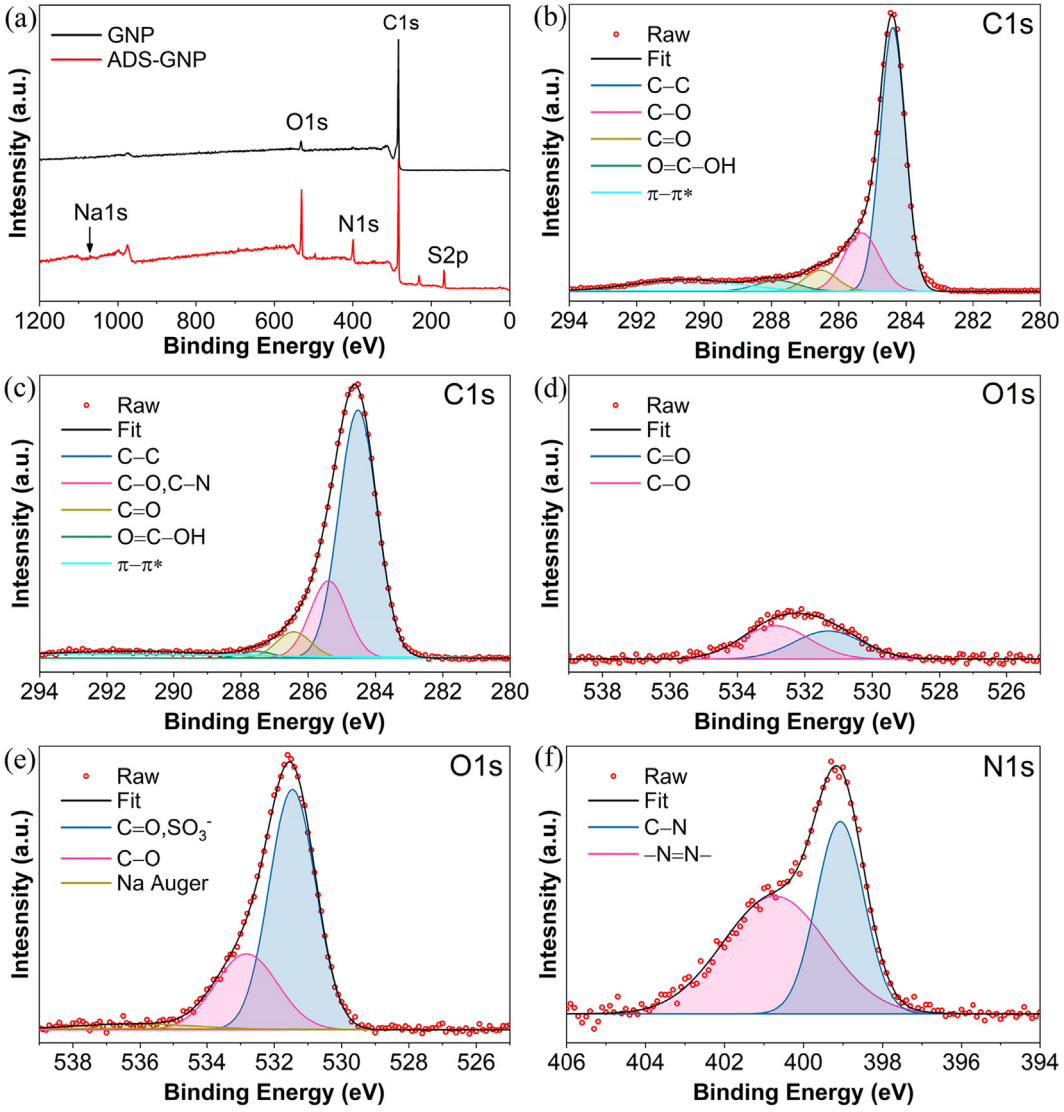

Fig. 3. (a) XPS survey of GNP and DS-GNP, C1s of (b) GNP, (c) DS-GNP, O1s of (d) GNP, (e) DS-GNP and N1s of (f) DS-GNP.

Table 2
Atomic concentration of detected elements from the XPS analysis.

Samples	C, at%	O, at%	N, at%	S, at%	Na, at%
GNP	95.72	4.28	n.d.	n.d.	n.d.
DS-GNP	67.29	17.36	10.37	4.53	0.45

uniformity with less heat loss. This thermal energy can pass through the external casing material first and exit through the other end [13–15]. There are several factors could influence the heat pipes efficiency including working pressure, inclination angle, filling ratio and nanoparticles concentration in the base fluid. The inclination angle (θ), defined as the angle between the heat pipe axis and the horizontal datum, of a heat pipe is of great importance especially for systems with spatial changing in position like solar heating systems and cooling devices. It is known that the inclination angle affects the thermal performance of thermosyphons and heat pipes utilizing traditional working fluids significantly. The filling ratio of the working fluid has a considerable effect on the heat transfer performance of thermosyphon and heat pipes. The filling ratio (FR) defined as the ratio of the working fluid volume to the evaporator section volume. However, they could not derive a clear trend with respect to different nanofluids. Moreover, the optimal filling ratios for nanofluids in heat pipes in most cases are the same or at least similar as for water [16]. Therefore, there has been an increasing interest in the use of heat pipes as a promising mean of cooling electronic devices as computer, electronic cards, telecommunication and satellite components [17]. The heat pipe working fluid can be selected from different fluids, depending on its compatibility with the shell and wick material, thermal conductivity, latent heat, thermal stability, surface tension and operating temperature. The various types of base fluid were used in the heat pipes including distilled water (DW), ethanol (C_2H_6O), acetone (C_3H_6O), the refrigerant R11 (trichlorofluoromethane, CCl_3F) and ethylene glycol. Recently, the classical working fluid of heat pipes were replaced with various types of nanofluids, therefore the transferred amount of heat can be increased due to the specific properties of nanofluids including thermal conductivity and specific heat transfer capacity [13,14,18]. Since the early 1990s, many studies have explored the utilization of various types of nanofluids as working fluids in heat pipes. The different types of nanoparticle material such as pure metals (i.e. nano gold, silver, copper and alumina), oxides (i.e. copper oxide), variations of carbon and most recently graphene were used in the heat pipes. Carbon based materials such as, graphene nanoplatelets (GNP), graphene oxide (GO), nitrogen-doped graphene (NDG) and etc. have drawn many applications such as heat transfer applications and composite materials due to their specific characteristics [19–22]. Table 1 is given, a summary of the recent experimental studies on heat pipe that

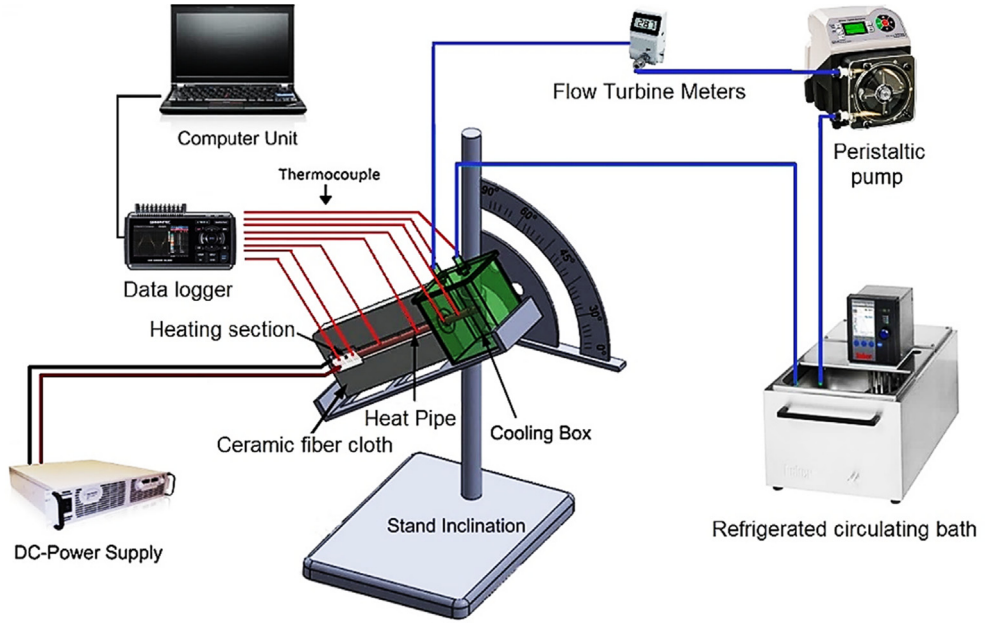

Fig. 4. Heat Pipe experimental setup for thermal performance evaluation.

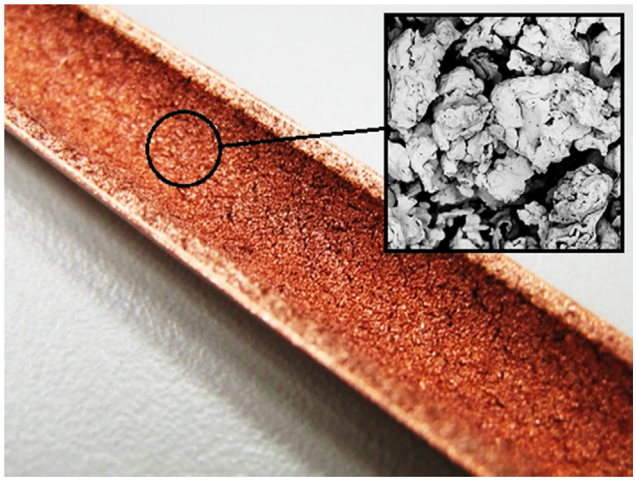

Fig. 5. Image of a copper powder sintered heat pipe (inset: SEM image of a sintered material).

filled with graphene nanofluid. These works showed that, the thermal performances of heat pipes with nanofluids were enhanced by reducing the thermal resistance [23].

The aim of this research work is the development specific nanofluid that could enhance the thermal performance and heat capacity of heat pipe. Graphene nanoplatelets (GNP) has attracted a lot of interest due to its superior thermal conductivity of 3000–5000 W/m.K and good mechanical properties [27]. Base on the literature [28], one of the most common working fluid with highest heat transfer capabilities that works in the low temperature region is water.

Facing the above literature, heat pipes can have a bright future in thermal engineering providing that more research is conducted to identify new carrying fluids with plausible heat transfer characteristics to further enhance the efficacy of the system. Therefore, in the present perusal, water soluble GNP was synthesized by covalent functionalization of GNP sheets with the diazonium salt (DS) of sodium 4-aminoazobenzene-4-sulfonate [29,30]. The DS was grafted to the surface of GNP through π–π interactions and covalent bonding [31]. It is expected that the hydrophilic functional groups of DS (sulfonic acid groups) could improve the dispersion stability of DS modified GNP (DS-GNP) [32]. Furthermore, DS-GNP nanofluid with different concentrations were implemented as working fluid to examine the effect of GNP sheet concentrations on heat transfer performances of heat pipe more thoroughly.

Table 3
Details of the experimental setup to evaluate the thermal performance of heat pipe.

Parameters	Details
Test section (heat pipe)	1. Cu Tube specification: Copper (JIS C1020) shell 2. Length (L): 300 mm 3. Outer Pipe Diameter (D_o): 8 mm 4. Wall Thickness: 0.5 mm Sintered Specification: 1. Cu powder: 63 μm 2. Porosity: 42% 3. Thickness: 1 mm
Evaporator section	Heating units was KEYSIGHT Technologies DC power supply
Condenser section	Including: 1. Cooling units was DAIHAN, Refrigerated Bath Circulator 2. Flow sensors (± 1% accuracy, OMEGA,) 3. Peristaltic pump (Longer pump)
Data recording system	Graphtec data logger (midi logger gl220)
Temperature data recording	It was started 600 s after temperature reached steady state (Approximately time between each heat input increment was 90 min)
Insulation method	All the heat pipe parts were wrapped with ceramic fibre cloth to minimize the heat loss
Heat pipe surface temperatures (T_1- T_5)	Thermocouple, type K (± 0.1 °C accuracy, OMEGA)
Inlet and outlet temperatures (T_{in} and T_{out})	Thermocouple, type K (± 0.1 °C accuracy, OMEGA)

2. Experimental method and process

2.1. Materials

Graphene nanoplatelets (GNP) Grade C, with specific surface area of 300 m^2/g was purchased from XG Sciences. $NaNO_2$ and hydrochloric acid (HCl, 37%) was bought from Merck Company. Sodium 4-

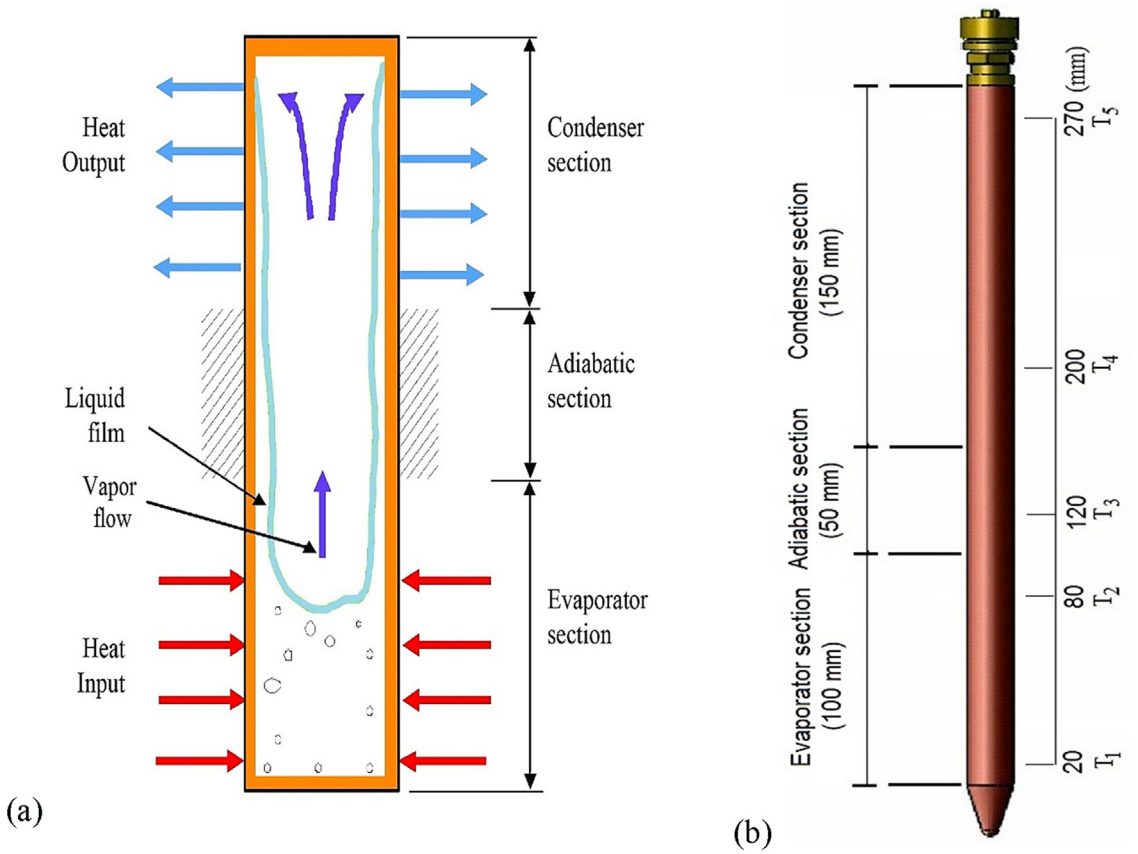

Fig. 6. (a) schematic cross section and (b) thermocouples locations on the surface of heat pipe.

Table 4
Uncertainty ranges analysis for heat pipes.

Parameters	Uncertainty range (%)
Temperature difference	0.1
Input heat	3.3
Input heat flux	3.2

aminoazobenzene-4-sulfonate was supplied by Tokyo Chemical Industry Co., Ltd. (TCI) that used to modify the surface of GNP.

2.2. Material preparation

To synthesize water soluble GNP, first DS was fabricated from reaction of 1.2 g of Sodium 4-aminoazobenzene-4-sulfonate with the mixture of 11 mL of DW, 5.5 mL of HCl and 0.32 g of $NaNO_2$ under continues stirring for 1 h in the 0 °C ice bath environment. Subsequently, 400 mg of GNP sheets was homogenized in 100 mL of DW by ultra-sonication probe for 5 min. Then, the prepared DS solution was gradually added to the GNP solution while stirring and temperature was maintained strictly below 5 °C using ice-water bath for 2 h. The reaction mixture was dialyzed using dialysis membrane for 14 days in DW. Finally, the blackish solution was added into the beaker and concentrations of covalent functionalized GNP nanofluid were maintained at volume percentage (φ) of 2, 3, 4 and 5%.

2.3. Characterization

The heat pipe sintered mesh microstructures of were examined by Field emission scanning electron microscopy (FE-SEM, CARL ZEISS AURIGA). X-ray photoemission spectrometer (XPS, PHI-Quantera II) with an Al-Ka (hm = 1486.8 eV) X-ray source was utilized to determine the functionalization of GNP.

The rheological behavior was determined using Anton Paar rheometer (Physica MCR 302). KD2 Pro has been utilized to evaluate the thermal conductivity of working fluid through heat needle method, (Decagon Devices, Inc., USA) with accuracy of %5 at a constant temperature. The stability of samples was by light transmission method with UV spectrophotometer (UV-2600, Shimadzu) that functioning between 190 and 1100 nm.

3. Results and discussion

GNP sheets were functionalized by diazonium salt using diazonium chemistry to synthesize water-dispersible GNP. A schematic of the diazonium reaction used to attach hydrophilic functional group to graphene sheets is shown in Fig. 1. Briefly, diazonium cations are prepared at acidic pH in the presence of $NaNO_2$ (Fig. 1a). Subsequently, GNP reduced the diazonium cation to aryl radical, which is responsible for the GNP functionalization (Fig. 1b) [30,33,34].

Today, most researchers have implemented ultrasonic waves to stabilize GNP nanoparticles in nanofluids to overcome the van der Waals interactions between the nanoparticles. In the present work, the prepared covalent functionalized nanoparticles are intended to disperse homogenously without using any external force, as shown in Fig. 2. This phenomenon is attributed to the existence of hydrophilic functional groups (sulfonic acid) of a modifier which attached to the surface of GNP. Furthermore, These GNP sheets possess excellent water dispersibility, as they started to disperse smoothly thereupon added to DW, without any aggregation.

3.1. Characterization of covalent functionalized GNP nanofluid

The elemental compositions of GNP and DS-G were analyzed via

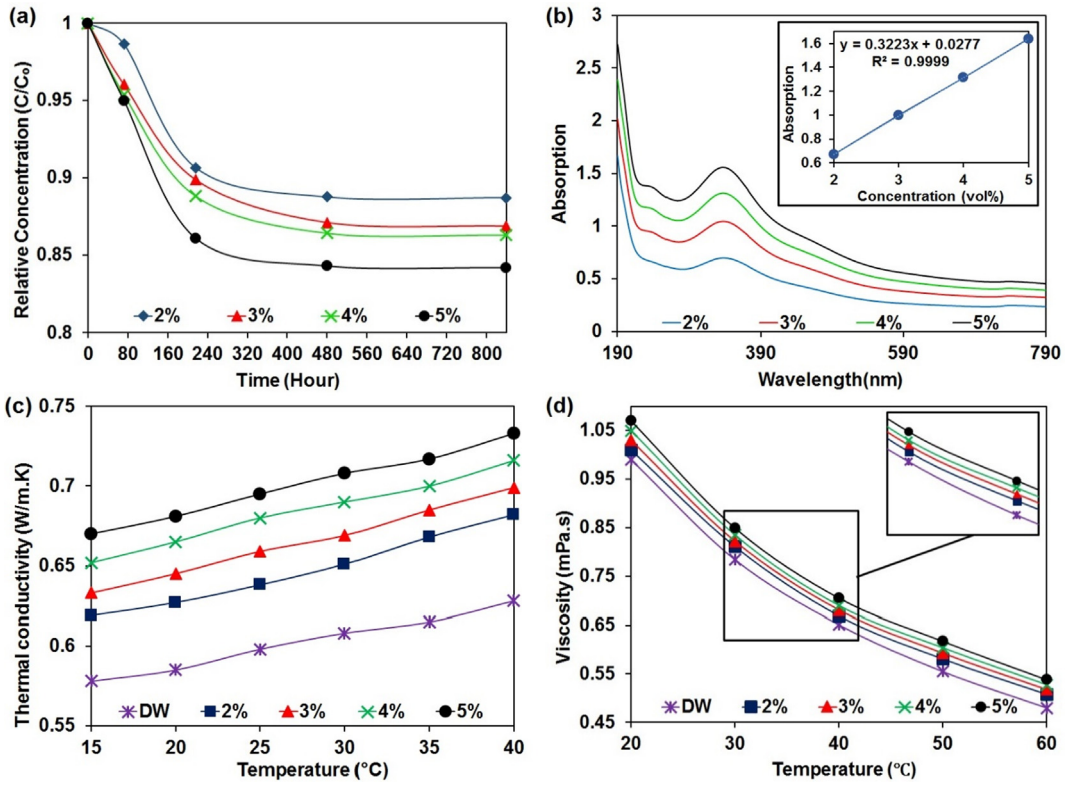

Fig. 7. (a) Relative concentration with sediment time; (b) UV–vis at different concentrations; (c) Thermal conductivity; (d) Viscosity profile of DS-GNP nanofluid.

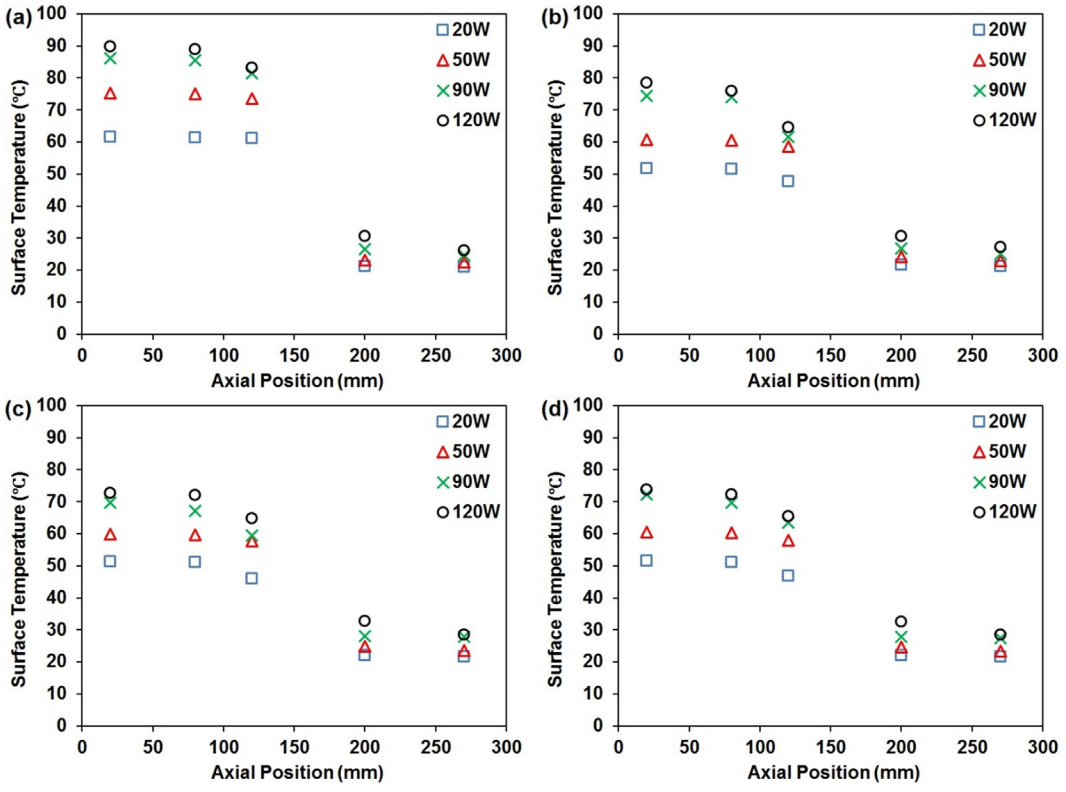

Fig. 8. Surface temperature distribution versus axial position for DW with 40% filling ratio at various inclination angles: (a) 0˚; (b) 30˚; (c) 50˚; (d) 70˚.

XPS. Fig. 3a shows XPS surveys of GNP and DS-GNP. The obvious N1s (399 eV) and S2p (167 eV) peaks appeared in DS-GNP compare with GNP. The C, O, S and N content in GNP and modified GNP as investigated by XPS are presented in Table 2. The appearance of the sulfur (sulfonate groups) and Nitrogen (azo groups), together with an increase in O (sulfonate groups), indicates the successful incorporation of the DS molecule onto the GNP [31,35].

C1s spectra of GNP and DS-GNP are presented in Fig. 3(b and c). In

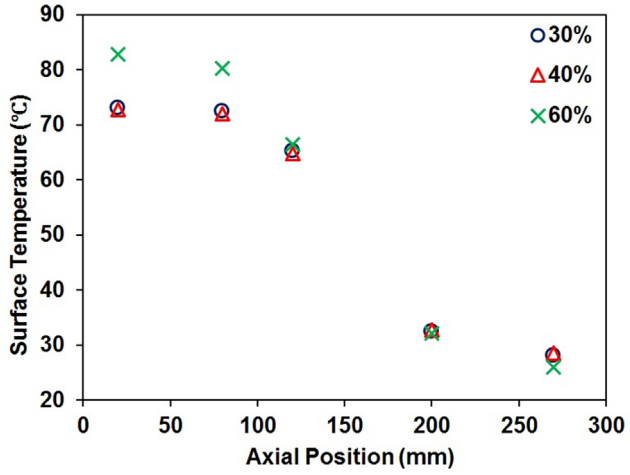

Fig. 9. Effect of filling ratio on the surface temperature distribution of heat pipe that charged with DW for 120 W and inclination angle of 50°.

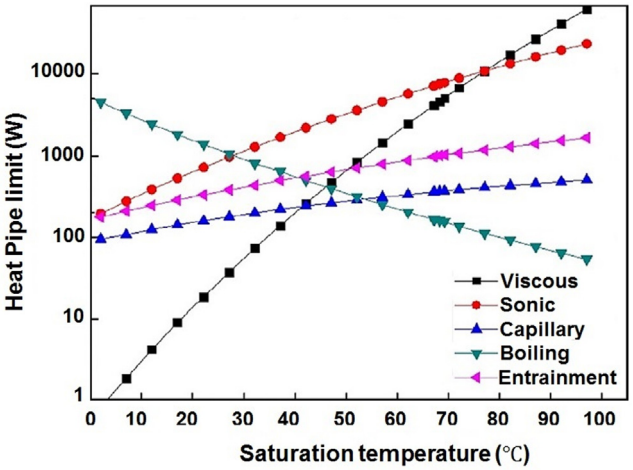

Fig. 10. Operation limit of heat pipe at filling ratio of 60% and inclination angle of 50°.

the C1s spectra of GNP the bands at 284.4, 285.5, 286.8, 287.9 and 290.5 eV belong to the C–C in the aromatic rings, C–O, C = O, O–C–OH and π–π* transition relative to aromatic carbon, respectively [29]. Upon functionalizing GNP, both the C–C content and the π–π* shake-up band decreased as a result of the disruption of the delocalized π conjugation in the graphitic structure [36]. In addition, the relative intensity of the band corresponding to the C–O or C–N groups increased in DS-GNP, which further confirms the successful functionalization of GNP by arylation with diazonium salts [35]. The O1s spectrum of GNP is deconvoluted into two bands at 531.3 (C = O) and 532.8 (C–O) eV (Fig. 3d). In the O1s spectrum of DS-GNP (Fig. 3e), the significant increase in the intensity of peak at 531.4 eV and appearance of new peak at 536.1 eV can be described by presence of oxygen atoms from the sulfonate functional group ($–SO_3^-$) and sodium ion (Na^+) of the attached DS [37]. Two peaks in the deconvoluted N1s spectrum of DS-GNP (Fig. 3f) at 399.1 and 400.5 eV are ascribed to the attachment of nitrogen atoms to the aromatic carbon rings (C–N) and azo radical groups (–N = N–), respectively [30,31,38]. All these observations support the successful grafting of DS on the GNP sheets during the diazonium functionalization (Fig. 1).

3.2. Heat pipe setup and experimental procedure

Fig. 4 represents the heat pipe experimental setup that consists of cooling and heating units, measurement instruments and an adjustable mounting platform.

Fig. 5 presents the image of the heat pipe as a test sections was made by copper material. Before experimental run, all the heat pipes were initially filled with the specific volume of working fluid that can be known as filling ratio and then there were evacuated by using a vacuum pump following by the sealing procedure. Thermal performance was investigated by using the DS-GNP nanofluid at different concentration ofφ = 2, 3, 4 and 5%. For each concentration, the heat pipes were charged with three filling ration (30, 40 and 60%) and performance of heat pipes were compared with the reference case of DW. Table 3 summarized the details of the experimental set up.

As shown in Fig. 6, Five K-type thermocouples (T_1 – T_5) were installed on outer surface of each heat pipe at the specific positions, which measured the evaporator, adiabatic and condenser section temperatures. The condenser section was submerged horizontally into the cooling chamber and a mixture of ethylene glycol (EG) and DW (60:40) as the coolant with 20 °C and 100 L/min flow rate was used for the cooling procedure. The input power to the evaporator section was adjusted from 20 W to 120 W and the inclination angle of heat pipe was maintained between 0° and 70°.

3.3. Data reduction

The heat pipe thermal resistance (R) is directly a proportion of temperature difference and given heat load that can be expressed as [10]:

$$R = \frac{T_e - T_c}{Q} \tag{1}$$

$$Q = VI \tag{2}$$

where T_c ($T_c = (T_4 + T_5)/2$) and T_e ($T_e = (T_1 + T_2)/2$) are the average temperature of condenser and evaporator, respectively. The heat transfer coefficient of evaporator (h_e) can be expressible as:

$$h_e = \frac{Q_e}{A_e \Delta T_e} \tag{3}$$

$$\Delta T_e = T_e - T_{vap} \tag{4}$$

where ΔT_e is the difference of temperature between the evaporator and the vapor ($T_{vap} = T_3$). The effective thermal conductivity is determined as:

$$k_{eff} = \frac{L_{eff}}{A_{cr} R} \tag{5}$$

where A_{cr}, R and L_{eff} are cross section area, thermal resistance and effective length of heat pipe, respectively.

$$L_{eff} = 0.5L_e + L_{ad} + 0.5L_c \tag{6}$$

where L_c, L_e, L_{ad} are condenser, evaporator and adiabatic sections length, respectively.

Thermal efficiency is the proportional of removed heat from condenser to the input heat into the evaporator and it can be given as:

$$\eta_{th} = \frac{Q_c}{Q} = \frac{(T_2 - T_1)}{Q} \tag{7}$$

where Q and Q_c are removed heat in the condenser and the input heat in the evaporator. $\dot{m}$ and c_p are the mass flow rate and specific heat of fluid in the evaporating cooling jacket, respectively. T_1 and T_2 are the temperature of inlet and outlet coolant.

The experimental test on the heat pips were conducted at different concentrations, heat inputs and inclination angles, as well as various filling ratios of the working fluids. The surface temperatures of heat pipes were recorded three times to confirm the reproducibility of the data. Table 4 illustrates the uncertainty analysis of the experiment [39].

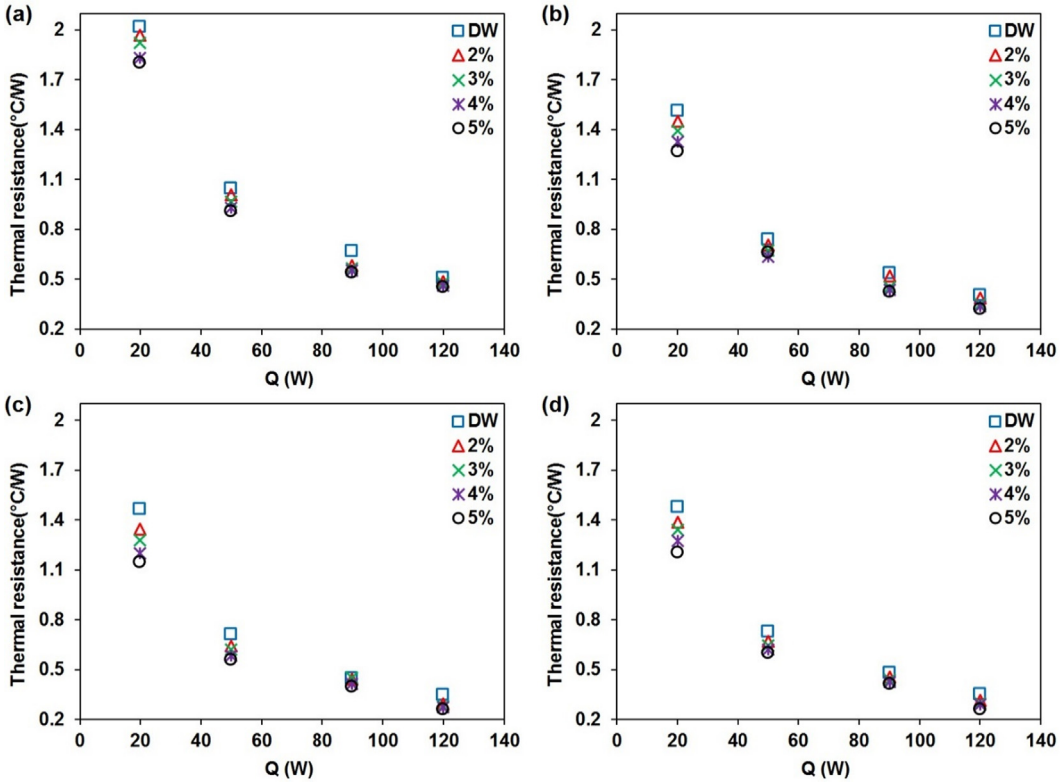

Fig. 11. Effect of applied parameters on the thermal resistance of heat pipe for optimum filling ratio (40%): (a) 0°; (b) 30°; (c) 50°; (d) 70°.

4. Results and discussion

4.1. Working fluid properties

The colloidal stability of working fluid is crucial in various applications and the relative concentration could be measure by UV–vis test. The light absorptions of nanofluids were directly related to the particles concentration and it could be explained by the Beer–Lambert's law [40]. The absorption wavelength decreases over time periods due to reduction of the nanofluid concentration (see inset of Fig. 7(b)). These observations suggest that the covalent functionalized GNP nanofluid has high dispersibility ratio. The reason is the existence of hydrophilic modifier (DS) attached to the GNP sheets which formed stable water dispersion. Fig. 7(a) illustrates the relative concentrations of DS-GNP nanofluid versus time span. It exhibited a maximum sedimentation of 16% after 480 hrs and it has remained steady up to 840 hrs. Therefore, this improvement for dispersibility of the GNP sheets in base fluid has a significant effect in the heat transfer characteristic of covalent functionalized GNP nanofluid.

To fully understand the impact of introducing functional groups to GNP on the thermal conductivity, the test was conducted for several concentrations and temperatures. The nanoparticles dispersion is complex behavior that defined in terms of Brownian model. The studies on thermal conductivity characteristics are important for several technological applications. Fig. 7(c) presents the thermal conductivity enhanced up to 17% by adding surface modified GNP sheets into the base fluid, which could be explained by Maxwell theory for this 2D material [41].

Fig. 7(d) shows rheological behavior of DS-GNP nanofluid and it behaves as Newtonian fluid. It could be seen that viscosity was changed with rise of temperature. Noticeably, this surface treated GNP sheets was considered to have low concentrations with minimal interactions among themselves. It should be mentioned that this behavior of DS-GNP nanofluid as a Newtonian fluid was measured above the shear rate of 200 s^{-1}.

4.2. Influence of different parameters on the heat pipe performances

Fig. 8 presents the surface temperature distribution profile of DW at filling ration of 40%. Based on the results, the heat pipe surface temperature reduced from evaporator part to condenser part. Furthermore, investigations on the different filling ratio and inclination angle were done to obtain the optimum condition that heat pipe has its highest performance. In Fig. 8, the surface temperature for $\theta = 50^{\circ}$ has the lowest amount, however it reached the dryout condition above 120 W with the horizontal ($\theta = 0^{\circ}$) positioning. The vapor and nanofluid inside the heat pipe move in different directions and the vapor pressure employs a shearing force on the working fluid at the interface point of vapor–liquid. Commonly, there are two main reason for dryout conditions of heat pipes. The first one happens, if magnitude of shearing force surpass the surface tension force of the fluid. Subsequently, working fluid droplets could be entrained into the vapor flow and these droplets will carry toward the condenser section. The power of this shearing force is related to the thermophysical properties and vapor velocity. Therefore, if the magnitude of shearing force exceeds the limitation and becomes large enough, it will induce dryout in the evaporator section. The second reason is entrainment limit that occurs at high vapor velocity and therefore, the droplets of working fluid in the wick are torn away from the wick surfaces and moved to the upper side with the vapor flow which causes dryout. Additionally, the surface temperature of the heat pipe is strongly influenced by inclination angle which is attributed to the wick capillary action between two ends of heat pipe.

The influence of filling ratio on the surface temperature distribution of heat pipe that filled with DW is shown in the Fig. 9. To study the filling ratio effect, heat pipes were loaded with various quantities of working fluids (30, 40 and 60%) at the several of inclination angle and input heat. The results show that the surface temperature of heat pipe decreased, when filling ratio of working fluid changes from 30% to 40%, followed by uprising in the surface temperature at the filling ratio of 60%. There are three main factors that can explain this phenomenon. The first factor is associated with the working fluid capacity, which is

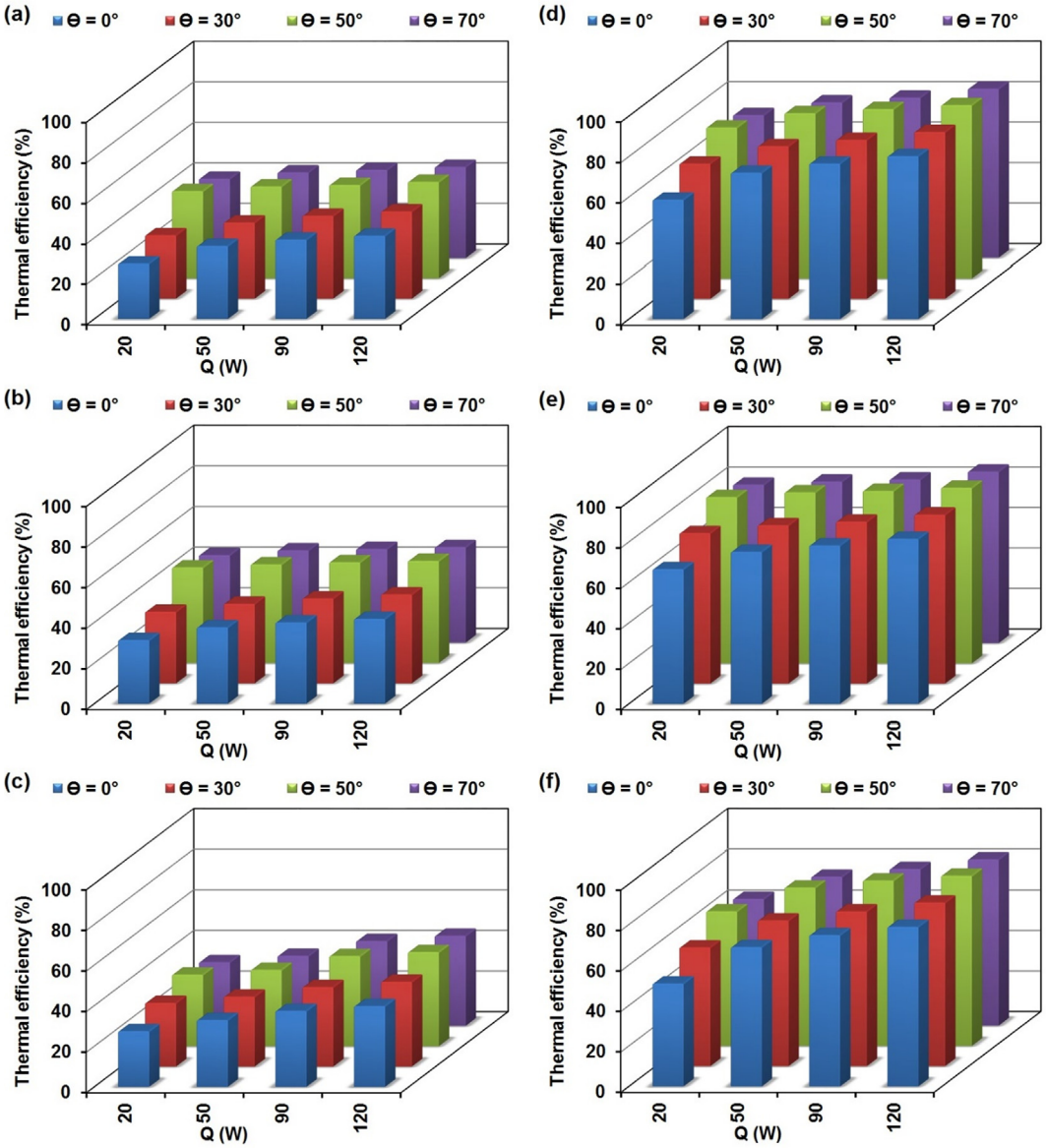

Fig. 12. Influence of filling ratio on the thermal efficiency of heat pipe at different input heat: (a) DW, 30%; (b) DW, 40%; (c) DW, 60%; (d)φ = 5%, 30%; (e)φ = 5%, 40%; (f)φ = 5%, 60%.

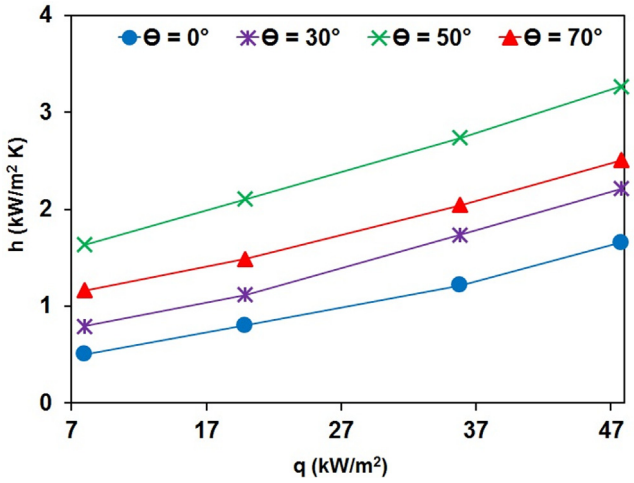

Fig. 13. Effect of inclination angle on average heat transfer coefficient atφ = 5% and filling ratio of 40%.

absorbing the heat. The second reason is the required space for carrying the generated vapor from the evaporator (hot zone) to condenser (cold zone) section as a results of working fluid phase change process. The last factor is pressure drop alongside of heat pipe. As a consequence of that, with more than 40% filling ratio, the total available volume inside the heat pipe reduced, which could influence the thermal efficiency of heat pipe.

The limitation of the sintered heat pipe filled with DW at the filling ratio of 60% was determined based on the literature [10,42]. Fig. 10 presents the analytical operation limits of heat pipe that filled with DW and it confirms that the limitation was highly relevant to the viscous limit, boiling limit and capillary.

Based on the results in Fig. 11, the thermal efficiency is at the optimum value with filling ratio of 40% at different inclination angles. The results suggest the reduction of thermal resistance versus the raise of input heat load for all of inclination angles. In Fig. 11, the inclination angle was the most effective parameter on the thermal resistance of heat pipes, which gradually decreased from 70° to 50° and then it increased from 50° to 0°. Based on the literatures [1,2] the movement of vapor inside the heat pipe from hot zone (evaporator) to cold zone

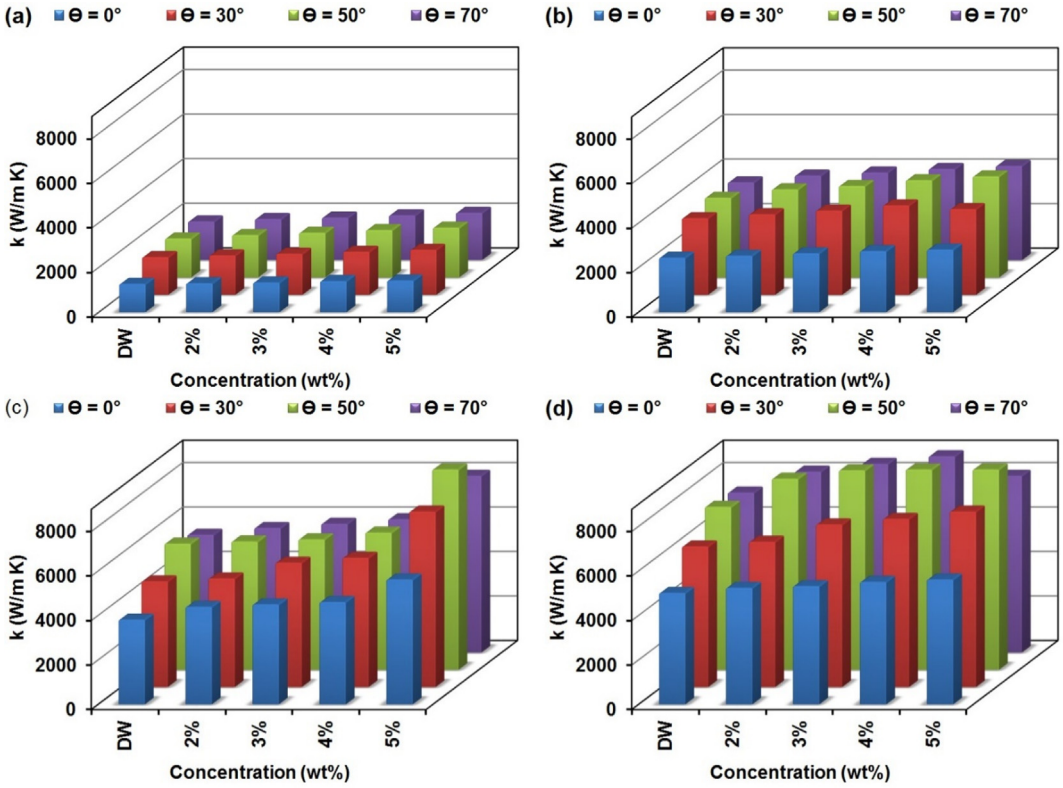

Fig. 14. Effective thermal conductivity of the heat pipe as a function of nanofluid concentration for several heating load: (a) 20 W, (b) 50 W, (c) 90 W, (d) 120 W.

(condenser) is due to the density difference between the two end of heat pipe. Therefore, condensed vapor returns to the evaporator from condenser as a result of the capillary action and gravity force. Subsequently, when the heat pipe inclination angle value exceeded 50˚, the thermal resistance increased upon the formation of a thick liquid film near the inner wall surface of the condenser section (Fig. 11). The maximum thermal resistance reduction was observed atφ = 5% by 26.4% compared with case of DW. It should be mentioned that deposition of nanoplatelets on the porous structure could create a coating in the evaporator section. This coating layer increases the surface wettability, thereby enhancing the thermal performance of the heat pipe.

To understand the influence of filling ratio on thermal efficiency of heat pipes, the heat pipes were loaded with different amount of working fluids including DW and DS-GNP nanofluid with concentration of φ = 5%. Fig. 12 illustrates the influence of filling ratio and different working fluid on the heat pipes thermal efficiency. Experimental results proved the enhancement of thermal efficiency in heat pipe, while filling ratio increased from 30% to 40%, however, it was decreased once the filling ratio changed to 60%. Totally, the thermal performance of heat pipe can be improved significantly by using nanofluids.

Fig. 13 shows the average heat transfer coefficient versus heat flux at concentration ofφ = 5% and optimum filling ratio (40%). The results clearly presented that the average heat transfer coefficient could be changed with the input heat flux and inclination angle. As presented in Fig. 13, the heat pipe average heat transfer coefficient reached the maximum at the inclination angle of 50˚. This phenomenon is due to the changes in the nucleate boiling heat transfer mechanism.

The copper has various advantages including its compatibility with low temperature working fluids and high thermal conductivity. In this case, it is beneficial to manufacture a high thermal conductive heat pipe for low and medium temperature applications. Based on the studies, performance of a heat pipe could be evaluated by measuring its effective thermal conductivity. This could be evaluated with Fourier's law for different geometries including squares or cylinders section. Fig. 14 presents the influence of inclination angles and input powers on the overall effective thermal conductivity with the optimum filling ratio. It shows that the maximum enhancement of effective thermal conductivity for nanofluid (φ = 5%), inclination angle of 50˚ and input heat of 120 W is 105% compared with the case of DW.

5. Conclusion

A systematic research work was done to prepare a highly stable graphene nanoplatelets (GNP) nanofluid followed by analysis of its capability as a working fluid in the heat pipe systems. The experiments were performed for the physical characterizations such as thermal conductivity, viscosity and stability of base fluid. The experimental results revealed that the DS functionalized GNP nanofluid has noticeable impact on thermal efficiency of heat pipes irrespective of inclination angle. The following conclusion remarks are drawn from this systematic study:

1- Highly water-soluble GNP was synthesized by covalent functionalization of GNP sheets with the diazonium salt (DS) of sodium 4-aminoazobenzene-4-sulfonate.
2- Thermal conductivity of nanofluid is enhanced up to 17% by adding surface modified GNP sheets in the base fluid.
3- It exhibited a maximum sedimentation of 16% after 480 hrs and it has remained steady up to 840 hrs.
4- The apparent enhancements of effective thermal conductivity (105%) and reduction in thermal resistance (26.4%) for DS-GNP nanofluid were indicated atφ = 5%.
5- It was clearly observed that the surface temperature decreased, when filling ratio of working fluid changed from 30% to 40% and then, the surface temperature was raised at the filling ratio of 60%.
6- The average heat transfer coefficient of heat pipe reached the maximum at the inclination angle of 50˚ due to the changing of the nucleate boiling heat transfer mechanism.
7- The inclination angle has a major impact on the thermal resistance

of heat pipes, which gradually decreased from 70° to 50° (optimum inclination angle).

Therefore, using this novel covalent functionalized GNP nanofluid as a heat pipe working fluid can improve its thermal efficiency and provides an opportunity for carrying more heat loads in the thermal management systems.

Declaration of Competing Interest

The authors declared that there is no conflict of interest.

Acknowledgements

The authors of the paper appreciate the Centre of Advanced Materials, School of Mechanical Engineering, University of Malaya for sharing their resources.

References

[1] M.M. Sarafraz, F. Hormozi, Experimental study on the thermal performance and efficiency of a copper made thermosyphon heat pipe charged with alumina–glycol based nanofluids, Powder Technol. 266 (2014) 378–387.
[2] S. Venkatachalapathy, G. Kumaresan, S. Suresh, Performance analysis of cylindrical heat pipe using nanofluids – An experimental study, Int. J. Multiph. Flow 72 (2015) 188–197.
[3] M. Gürü, A. Sözen, U. Karakaya, E. Çiftçi, Influences of bentonite-deionized water nanofluid utilization at different concentrations on heat pipe performance: An experimental study, Appl. Therm. Eng. 148 (2019) 632–640.
[4] Z.-H. Liu, B.-C. Zheng, Q. Wang, S.-S. Li, Study on the thermal storage performance of a gravity-assisted heat-pipe thermal storage unit with granular high-temperature phase-change materials, Energy 81 (2015) 754–765.
[5] B. Zohuri, Heat pipe design and technology: A practical approach, CRC Press, 2011.
[6] K.M. Kim, I.C. Bang, Effects of graphene oxide nanofluids on heat pipe performance and capillary limits, Int. J. Therm. Sci. 100 (2016) 346–356.
[7] M. Khalili, M.B. Shafii, Experimental and numerical investigation of the thermal performance of a novel sintered-wick heat pipe, Appl. Therm. Eng. 94 (2016) 59–75.
[8] E. Sadeghinezhad, H. Togun, M. Mehrali, P. Sadeghi Nejad, S. Tahan Latibari, T. Abdulrazzaq, S.N. Kazi, H.S.C. Metselaar, An experimental and numerical investigation of heat transfer enhancement for graphene nanoplatelets nanofluids in turbulent flow conditions, Int. J. Heat Mass Transf. 81 (2015) 41–51.
[9] C. Zhang, F. Yu, X. Li, Y. Chen, Gravity–capillary evaporation regimes in microgrooves 65 (2019) 1119–1125.
[10] M. Mehrali, E. Sadeghinezhad, R. Azizian, A.R. Akhiani, S. Tahan Latibari, M. Mehrali, H.S.C. Metselaar, Effect of nitrogen-doped graphene nanofluid on the thermal performance of the grooved copper heat pipe, Energy Convers. Manage. 118 (2016) 459–473.
[11] A. Takawale, S. Abraham, A. Sielaff, P.S. Mahapatra, A. Pattamatta, P. Stephan, A comparative study of flow regimes and thermal performance between flat plate pulsating heat pipe and capillary tube pulsating heat pipe, Appl. Therm. Eng. 149 (2019) 613–624.
[12] M. Ghanbarpour, N. Nikkam, R. Khodabandeh, M.S. Toprak, M. Muhammed, Thermal performance of screen mesh heat pipe with Al_2O_3 nanofluid, Exp. Therm Fluid Sci. 66 (2015) 213–220.
[13] S.-C. Wong, H.-H. Tseng, S.-H. Chen, Visualization experiments on the condensation process in heat pipe wicks, Int. J. Heat Mass Transf. 68 (2014) 625–632.
[14] L.-L. Jiang, Y. Tang, H.-Y. Wu, W. Zhou, L.-Z. Jiang, Fabrication and thermal performance of grooved-sintered wick heat pipe, J. Central South Univ. 21 (2014) 668–676.
[15] X. Liu, Y. Chen, M. Shi, Dynamic performance analysis on start-up of closed-loop pulsating heat pipes (CLPHPs), Int. J. Therm. Sci. 65 (2013) 224–233.
[16] W.I.A. Aly, M.A. Elbalshouny, H.M. Abd El-Hameed, M. Fatouh, Thermal performance evaluation of a helically-micro-grooved heat pipe working with water and aqueous Al2O3 nanofluid at different inclination angle and filling ratio, Appl. Therm. Eng. 110 (2017) 1294–1304.
[17] K. Zeghari, H. Louahlia, S. Le Masson, Experimental investigation of flat porous heat pipe for cooling TV box electronic chips, Appl. Therm. Eng. 163 (2019) 114267.
[18] M. Mehrali, E. Sadeghinezhad, M.A. Rosen, S. Tahan Latibari, M. Mehrali, H.S.C. Metselaar, S.N. Kazi, Effect of specific surface area on convective heat transfer of graphene nanoplatelet aqueous nanofluids, Exp. Therm Fluid Sci. 68 (2015) 100–108.
[19] V. Chandra, J. Park, Y. Chun, J.W. Lee, I.-C. Hwang, K.S. Kim, Water-dispersible magnetite-reduced graphene oxide composites for arsenic removal, ACS Nano 4 (2010) 3979–3986.
[20] E. Sadeghinezhad, M. Mehrali, R. Saidur, M. Mehrali, S. Tahan Latibari, A.R. Akhiani, H.S.C. Metselaar, A comprehensive review on graphene nanofluids: Recent research, development and applications, Energy Convers. Manage. 111 (2016) 466–487.
[21] E. Sadeghinezhad, M. Mehrali, S. Tahan Latibari, M. Mehrali, S.N. Kazi, S. Oon, H.S.C. Metselaar, Experimental investigation of convective heat transfer using graphene nanoplatelet based nanofluids under turbulent flow conditions, Ind. Eng. Chem. Res. 53 (2014) 12455–12465.
[22] M. Mehrali, E. Sadeghinezhad, M. Rashidi, A. Akhiani, S. Tahan Latibari, M. Mehrali, H. Metselaar, Experimental and numerical investigation of the effective electrical conductivity of nitrogen-doped graphene nanofluids, J. Nanopart. Res. 17 (2015) 1–17.
[23] R. Zhou, S. Fu, H. Li, D. Yuan, B. Tang, G. Zhou, Experimental study on thermal performance of copper nanofluids in a miniature heat pipe fabricated by wire electrical discharge machining, Appl. Therm. Eng. 160 (2019) 113989.
[24] L.G. Asirvatham, S. Wongwises, J. Babu, Heat transfer performance of a glass thermosyphon using graphene–acetone nanofluid, J. Heat Transfer 137 (2015) 111502 111502.
[25] T. Tharayil, L.G. Asirvatham, V. Ravindran, S. Wongwises, Thermal performance of miniature loop heat pipe with graphene–water nanofluid, Int. J. Heat Mass Transf. 93 (2016) 957–968.
[26] X. Su, M. Zhang, W. Han, X. Guo, Enhancement of heat transport in oscillating heat pipe with ternary fluid, Int. J. Heat Mass Transf. 87 (2015) 258–264.
[27] M. Mehrali, E. Sadeghinezhad, M.A. Rosen, A.R. Akhiani, S. Tahan Latibari, M. Mehrali, H.S.C. Metselaar, Heat transfer and entropy generation for laminar forced convection flow of graphene nanoplatelets nanofluids in a horizontal tube, Int. Commun. Heat Mass Transfer 66 (2015) 23–31.
[28] M. Ghanbarpour, N. Nikkam, R. Khodabandeh, M.S. Toprak, Thermal performance of inclined screen mesh heat pipes using silver nanofluids, Int. Commun. Heat Mass Transfer 67 (2015) 14–20.
[29] D.S. Yu, T. Kuila, N.H. Kim, P. Khanra, J.H. Lee, Effects of covalent surface modifications on the electrical and electrochemical properties of graphene using sodium 4-aminoazobenzene-4′-sulfonate, Carbon 54 (2013) 310–322.
[30] J. Greenwood, T.H. Phan, Y. Fujita, Z. Li, O. Ivasenko, W. Vanderlinden, H. Van Gorp, W. Frederickx, G. Lu, K. Tahara, Y. Tobe, H. Uji-i, S.F.L. Mertens, S. De Feyter, Covalent modification of graphene and graphite using diazonium chemistry: tunable grafting and nanomanipulation, ACS Nano 9 (2015) 5520–5535.
[31] D.S. Yu, T. Kuila, N.H. Kim, J.H. Lee, Enhanced properties of aryl diazonium salt-functionalized graphene/poly (vinyl alcohol) composites, Chem. Eng. J. 245 (2014) 311–322.
[32] M. Jana, P. Khanra, N.C. Murmu, P. Samanta, J.H. Lee, T. Kuila, Covalent surface modification of chemically derived graphene and its application as supercapacitor electrode material, PCCP 16 (2014) 7618–7626.
[33] S. Mahouche-Chergui, S. Gam-Derouich, C. Mangeney, M.M. Chehimi, Aryl diazonium salts: a new class of coupling agents for bonding polymers, biomacromolecules and nanoparticles to surfaces, Chem. Soc. Rev. 40 (2011) 4143–4166.
[34] C.R. Ryder, J.D. Wood, S.A. Wells, Y. Yang, D. Jariwala, T.J. Marks, G.C. Schatz, M.C. Hersam, Covalent functionalization and passivation of exfoliated black phosphorus via aryl diazonium chemistry, Nat. Chem. 8 (2016) 597.
[35] F. Sordello, G. Zeb, K. Hu, P. Calza, C. Minero, T. Szkopek, M. Cerruti, Tuning TiO2 nanoparticle morphology in graphene–TiO2 hybrids by graphene surface modification, Nanoscale 6 (2014) 6710–6719.
[36] M.M. Bernal, A. Di Pierro, C. Novara, F. Giorgis, B. Mortazavi, G. Saracco, A. Fina, Edge-grafted molecular junctions between graphene nanoplatelets: applied chemistry to enhance heat transfer in nanomaterials, Adv. Funct. Mater. 28 (2018) 1706954.
[37] S. Fleutot, H. Martinez, J.-C. Dupin, I. Baraille, C. Forano, G. Renaudin, D. Gonbeau, Experimental (X-Ray Photoelectron Spectroscopy) and theoretical studies of benzene based organics intercalated into layered double hydroxide, Solid State Sci. 13 (2011) 1676–1686.
[38] Y. Feng, H. Liu, W. Luo, E. Liu, N. Zhao, K. Yoshino, W. Feng, Covalent functionalization of graphene by azobenzene with molecular hydrogen bonds for long-term solar thermal storage, Sci. Rep. 3 (2013) 3260.
[39] J.R. Taylor, An introduction to error analysis: the study of uncertainties in physical measurements, University science books, 1997.
[40] S. Iranmanesh, M. Mehrali, E. Sadeghinezhad, B.C. Ang, H.C. Ong, A. Esmaeilzadeh, Evaluation of viscosity and thermal conductivity of graphene nanoplatelets nanofluids through a combined experimental–statistical approach using respond surface methodology method, Int. Commun. Heat Mass Transfer 79 (2016) 74–80.
[41] M. Mehrali, E. Sadeghinezhad, S. Tahan Latibari, M. Mehrali, H. Togun, M.N.M. Zubir, S.N. Kazi, H. Metselaar, Preparation characterization, viscosity, and thermal conductivity of nitrogen-doped graphene aqueous nanofluids, J. Mater. Sci. 49 (2014) 7156–7171.
[42] I.G. Kim, K.M. Kim, Y.S. Jeong, I.C. Bang, Performance of annular flow path heat pipe with a polymer insert controlling compactness for energy applications, Int. J. Heat Mass Transf. 92 (2016) 929–939.